



The use of D-optimal design to model the effects of process parameters on mineralization and discoloration kinetics of Fenton-type oxidation

Ivana Grčić*, Dinko Vujević, Natalija Koprivanac

Faculty of Chemical Engineering and Technology, Department of Polymer Engineering and Organic Chemical Technology, University of Zagreb, Marulićev Trg 19, HR-10000, Zagreb, Croatia

ARTICLE INFO

Article history:

Received 6 March 2009

Received in revised form

20 November 2009

Accepted 23 November 2009

Keywords:

Wastewater treatment

Reactive dyes

Fenton oxidation

D-optimal design

ABSTRACT

The aim of this experimental investigation was to study kinetics of Fenton and modified Fenton oxidation applied to miscellaneous dye solutions. Several bench scale laboratory tests for the treatment of colored wastewaters containing model pollutant compounds, reactive azo dyes C.I. Reactive Violet 2 (RV2) and C.I. Reactive Yellow 3 (RY3) were performed. In order to examine the effects of initial Fe^{2+} concentration, oxidant/catalyst molar ratio and oxidant type on TOC reduction and color removal, the following reactants were used: classic Fenton's reagent ($\text{Fe}^{2+}/\text{H}_2\text{O}_2$) and modified Fenton's reagent, where potassium peroxodisulfate, alone and in combination with hydrogen peroxide, was selected as oxidant. Response surface methodology (RSM), particularly D-optimal design, was used for the purpose.

This research contributed in several ways: (i) evaluation of more effective Fenton oxidant on pollutant content reduction, in terms of TOC and color removal, (ii) assessment of the optimal reactant doses, (iii) describing the RV2 kinetic behavior in applied systems and (iv) determining the apparent rate constants. Mineralization was described by pseudo-first-order kinetics with observed rate constant $k_m = 0.0133 \text{ min}^{-1}$. A kinetic model describing discoloration was composed of two first-order in-series reactions with discoloration rates; $k_1 = 0.9447 \text{ min}^{-1}$ and $k_2 = 0.0236 \text{ min}^{-1}$, at optimal operating conditions and with the highest initial organic load.

© 2009 Elsevier B.V. All rights reserved.

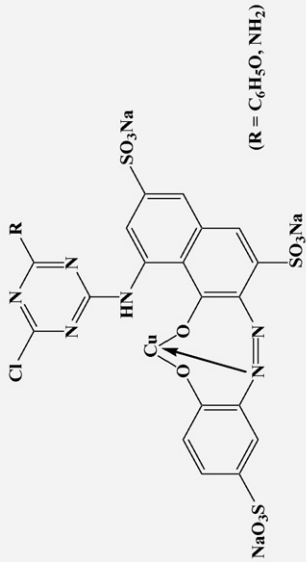
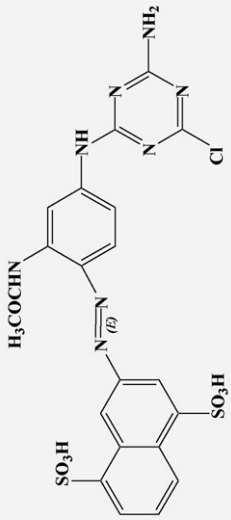
1. Introduction

Wastewaters originated from dye manufacturing and textile industries or by those related to dye consumption are usually loaded with significant quantities of dyes, causing the coloration of waste streams visible even in concentrations such as 1 mg L^{-1} . Hence, a small amount of such effluents discharged into water bodies might significantly change the color of rivers or lakes inhibiting the transmission of natural light and consequently present a hazard to aquatic ecosystems together with the increase of loading of organic content [1–3]. Among all dyes produced today a group of reactive dyes participates with a large portion and becomes the most remarkable due to specific characteristics of linkage between colorant and natural fibers. It is estimated that 15% of the world's dye production end up in the environment during the manufacturing and application processes [1]. Furthermore, many synthetic organic dyes and their metabolites are toxic, carcinogenic and mutagenic and pose a potential health hazard to humankind [4]. Due to this fact and rapid development and implementation of more and more stringent environmental reg-

ulations [5], convenient methods for the treatment of different types of colored wastewater have been a subject of a strong interest in recent years [3,6,7]. Generally, methods for the colored wastewater treatment can be grouped as biological, physical and chemical methods [8]. Biological methods have been widely used for the treatment of municipal and industrial wastewater. Despite of the lot of advantages, due to the complex aromatic structure and stability of reactive dyes, conventional biological treatment methods are ineffective for the structure degradation. Physical methods of wastewater treatment (adsorption, flocculation/coagulation, membrane processes, and ion exchange) [9–13], generally present transfer of pollution from one phase to the other, often expensive and not enough eco-efficient. Formation of secondary waste disposal and adsorbents regeneration additionally decreases economical efficiency of these processes. The alternative to the conventional colored wastewater treatment processes presents advanced oxidation processes (AOPs) that can be applied individually or as a part of integral treatment process [14]. The advantage of these processes in comparison with conventional wastewater treatment methods is the possibility of complete degradation of organic load towards water, carbon dioxide, nitrates, sulfates and chlorides. Advanced oxidation processes include formation of highly reactive species (radicals) under the chemical, electrical or radioactive energy and react non-selectively with per-

* Corresponding author. Tel.: +385 1 4597 123; fax: +385 1 4597 143.
E-mail address: igrcic@fkit.hr (I. Grčić).

Table 1
Structure and absorptivities of selected reactive dyes at studied wavelengths.

Dye	Structure	Molar extinction coefficient, $\text{cm}^{-1}\cdot\text{L}\cdot\text{mol}^{-1}$
C.I. Reactive Violet 2 (RV2)	 $(R = \text{C}_6\text{H}_4\text{O}, \text{NH}_2)$	385 nm 550 nm 120 16,000
C.I. Reactive Yellow 3 (RY3)		13,000 0

sistent organic compounds transferring them into by-products which are not always harmless but can be degraded much more easily [2,10]. These species have high redox potential and one of the most important is hydroxyl radical (2.8V). It can attack and destruct organic compounds towards water and carbon dioxide, i.e. mineralize it completely [15,16]. Depending on the hydroxyl radical generation, different types of AOPs are known, such as Fenton and Fenton “like” processes, UV photolysis, UV peroxone process, TiO_2 photo-catalysis, high voltage electrical discharge, radiolysis, γ -radiation. Fenton process is based on oxidation with Fenton reagent which presents an oxidative mixture of hydrogen peroxide and ferrous ions (Fe^{2+}) as catalyst. The efficiency of Fenton process depends on: concentration of ferrous (Fe^{2+}) and hydrogen peroxide Eq. (1), their molar ratio, pH of the system and temperature [3,8]



Peroxodisulfate is the most recent form of oxidant agent being used for environmental applications in the field of water and soil remediation. Sodium peroxodisulfate ($\text{Na}_2\text{S}_2\text{O}_8$) is the most commonly used form of peroxodisulfate salt, as the low solubility of potassium peroxodisulfate ($\text{K}_2\text{S}_2\text{O}_8$) limits its application as remediation agent [17,18]. Peroxodisulfate salts dissociate in water to peroxodisulfate anions ($\text{S}_2\text{O}_8^{2-}$), which, although strong oxidants (standard redox potential about 2.0V), are kinetically slow in destroying the majority of the organic pollutants. Like in the case of modified Fenton’s reagent, the addition of transition metal ions (e.g. ferrous ion) could activate the peroxodisulfate anion ($\text{S}_2\text{O}_8^{2-}$) to produce a powerful oxidant known as the sulfate free radical ($\text{SO}_4^{\bullet-}$), Eq. (2). Sulfate free radicals have a standard redox potential of 2.6V and may be able to oxidize many organic pollutants [19]. In the presence of hydroxyl radicals, peroxodisulfate free radicals could be generated [20,21], Eq. (3):



The experience in scientific research of application of peroxodisulfate as modified Fenton’s reagent for dye wastewater treatment is currently very limited.

In the context of developing the mathematical models that describes the effects of process parameters on process performance and chemical kinetics, experimental designs are often common practice. Response surface methodology (RSM) is important branch of experimental design. It is a critical technology in developing new processes and optimizing their performance. It is often an important concurrent engineering tool in process development because the objectives of process performance improvement can often be accomplished directly using RSM [22,23]. RSM design is a helpful tool for quantification of the relationships between one or more measured responses and the vital input factors. Regarding the general model structure of a response surface, Eq. (4):

$$Y = bX + \varepsilon \quad (4)$$

where Y , X , b , and ε are the matrices of response, coefficients to be estimated, independent variable levels, and errors, respectively; an optimal experimental plan can be computed by using the methodology of optimal experimental design for parameter estimation [24]. D-optimal criterion, one of the several “alphabetic” optimalities [22], was developed to select design points in a way that minimizes the variance associated with the estimates of specified model coefficients [25]. D-optimal design assumes a wide choice of “candidate” points and an adequate coverage of design space.

The scope of this study was to evaluate the application of Fenton-type processes ($\text{Fe}^{2+}/\text{H}_2\text{O}_2$, $\text{Fe}^{2+}/\text{H}_2\text{O}_2 + \text{K}_2\text{S}_2\text{O}_8$ and $\text{Fe}^{2+}/\text{K}_2\text{S}_2\text{O}_8$) for the treatment of colored wastewaters containing model pollutant compounds, reactive azo dyes C.I. Reactive

Table 2
Actual factors and their levels.

Parameter name	Code	Levels				
		1	2	3	4	5
		Numerical				
		–1	–0.33	0	+0.33	+1
		Categorical				
		0	1	2		
Initial ferrous ions concentration, [Fe ²⁺], mmol L ⁻¹	X ₁	0.25	0.83	1.13	1.42	2.00
Oxidant/catalyst molar ratio, ox/Fe	X ₂	5.00	20.00	27.50	35.00	50.00
Initial RY3 concentration, γ _{RY3} , mg L ⁻¹	X ₃	10.00	23.33	30.00	36.67	50.00
Type of oxidant	X ₄	H ₂ O ₂	H ₂ O ₂ + K ₂ S ₂ O ₈ (1:1)	K ₂ S ₂ O ₈		

Violet 2 (RV2) and C.I. Reactive Yellow 3 (RY3). Model solution of Reactive azo dye, C.I. Reactive Violet 2 (RV2), was replenished with other reactive azo dye, C.I. Reactive Yellow 3 (RY3). In order to evaluate the effect of the presence of another similar organic pollutant on RV2 degradation extent and apparent discoloration rate, concentration of RY3 was varied. Furthermore, the effects of initial Fe²⁺ concentration, oxidant/catalyst molar ratio and oxidant type on TOC and color removal, and the apparent mineralization and discoloration rate constants were studied. The efficiency of the processes was determined by: (i) observing the mineralization extent based on total organic carbon (TOC) analysis, and (ii) monitoring color removal based on UV–vis spectrophotometry. Also, the kinetics of mineralization and discoloration was investigated. The statistical study of the studied system was performed applying RSM D-optimal design, and adequate statistical predictive models were developed.

2. Materials and methods

2.1. Chemicals

All reagents used in this work were analytical reagent grade and used without any further purification. Ferrous sulfate (FeSO₄·7H₂O), hydrogen peroxide (30%, w/w) and potassium peroxodisulfate (K₂S₂O₈) used in this work were supplied by Kemika, Zagreb, Croatia, and ferric sulfate [Fe₂(SO₄)₃·9H₂O] by Alkaloid, Skopje, Macedonia. C.I. Reactive Violet 2 (RV2) and C.I. Reactive Yellow 3 (RY3) (Table 1) were obtained from Ciba-Geigy, Basel, Switzerland as a free of charge samples. Experiments were performed using model dye wastewater of RV2 (50 mg L⁻¹) replenished with RY3 in the concentration range from 10 to 50 mg L⁻¹. The initial pH of the studied system was adjusted at 3 using sulfuric acid (c = 1 mol L⁻¹), which was followed by the addition of ferrous sulfate.

2.2. Performing the experiments

All experiments were performed as bench scale tests in 120 mL glass reaction vessels with the reaction volume of 100 mL and constant magnetic stirring (600 rpm), at room temperature, 23 ± 2 °C. Samples were taken out in certain periods of time within 30 min and subjected to further analyses. Mineralization extents were determined on the basis of total organic carbon (TOC) content measurements, performed by using total organic carbon analyzer; TOC-V_{C_{PN}} 5000 A, Shimadzu. A Perkin–Elmer Lambda EZ 201 UV/VIS spectrophotometer was used for discoloration monitoring at λ_{max} = 385 and 550 nm, i.e. the wavelengths of maximum for an each dye.

2.3. Experimental design and statistical analysis

A four factor (three numerical plus one categorical) D-optimal design was used to determine the operating conditions for max-

imizing the mineralization and discoloration. Based on previous experience in related works [26,27], (X₁) initial Fe²⁺ concentration, (X₂) oxidant/catalyst molar ratio, i.e. ox/Fe (X₃) initial RY3 concentration and (X₄) type of oxidant, H₂O₂, H₂O₂ + K₂S₂O₈ (1:1) or K₂S₂O₈, were chosen as the four factors for investigation (Table 2). These parameters (X₁, X₂, X₃, X₄) are identified as control factors (CFs) because the variation of their values results in optimal performance. Other parameters, i.e. pH, temperature and stirring velocity were set at fixed values. Evaluation of the Fenton process in terms of pH value has already been performed and published [28,29].

The method consisted of (i) defining levels, (ii) selection of the model that fits, (iii) choosing design points, *h*, from the set of *n* candidate points generated depending on the selected model. As presented in Table 2, numeric factors are varied over 5 levels, while categorical factor contains 3 levels, i.e. three categories. D-optimal design as a technique demands selections of the model at the beginning. That could be difficult if there were no expectations of what model should be. In this particular case, there is some allusion about the model [27,30]. So, a reduced cubic model was selected, Eq. (5)

$$Y = b_0 + b_1X_1 + b_2X_2 + b_3X_3 + b_4X_4 + b_{12}X_1X_2 + b_{13}X_1X_3 + b_{14}X_1X_4 + b_{23}X_2X_3 + b_{24}X_2X_4 + b_{34}X_3X_4 + b_{124}X_1X_2X_4 \quad (5)$$

where *b_n* is the coefficient associated with each *n*th factor, and the letters, X₁, X₂, X₃, X₄ represent the factors in the model. Combination of factors (such as X₁X₂) represents interactions between the individual factors in that term.

Regarding the selected model, for the given combination of the *k* factors, a set of *n* candidate points (285) was generated. The objective of D-optimal design is to select *h* design points from that set by embedded algorithm, which resulted in 17 minimum model points, *k* + 1 (5) points for estimation of lack-of-fit and replicates as well. Finally, an experimental plan with total of 27 experiments was made (Table 3). Table 3 shows the standard array for four factors and 27 experiments. It also shows the run order and the observed responses. The experiments were performed in a random manner in order to avoid any systematic bias in the outcomes.

Obtained model was evaluated for each response function and the experimental data (TOC and color removal, the apparent mineralization and discoloration rate constants) were analyzed statistically applying analysis of variance (ANOVA) and using *Design-Expert 6.0.6*, a DoE software tool from Stat-Ease, Inc. The adequacy of the final model was verified by graphical and numerical analysis.

3. Results and discussion

3.1. Spectrophotometric data

Miscellaneous dye solution of RV2 (50 mg L⁻¹) and of RY3 in concentrations varied from 10 to 50 mg L⁻¹, was studied as stated previously. In such systems, the changes in concentration of studied dyes were easy to monitor due to the fact that both dyes showed

Table 3
Design matrix and responses.

Std	Run	Numeric factors			Categorical factor (X ₄) type of oxidant	Responses					
		(X ₁) [Fe ²⁺], mmol L ⁻¹	(X ₂) ox/Fe molar ratio	(X ₃) γ _{RY3} , mg L ⁻¹		(Y ₁) (TOC ₀ -TOC ₃₀) ·100/TOC ₀ , %	(Y ₂) k _m , min ⁻¹	(Y ₃) (Abs _{385nm,0} - Abs _{385nm,30}) ·100/Abs _{385nm,0} , %	(Y ₄) (Abs _{550nm,0} - Abs _{550nm,30}) ·100/Abs _{550nm,0} , %	(Y ₅) k ₁ , min ⁻¹	(Y ₆) k ₂ , min ⁻¹
23	1	2.00	50.00	10.00	K ₂ S ₂ O ₈	12.8	0.0041	2.6	98	0.5	0.0522
11	2	0.25	5.00	10.00	K ₂ S ₂ O ₈	8.1	0.0029	-15.4	92.8	0.2733	0.0491
24	3	0.25	5.00	10.00	H ₂ O ₂	24	0.0106	68	99.5	0.7636	0.0519
18	4	1.13	27.50	30.00	H ₂ O ₂	28.4	0.0136	69.1	99.4	0.774	0.0446
4	5	0.25	50.00	10.00	H ₂ O ₂	32.2	0.0125	74.7	99.8	0.8127	0.0806
9	6	0.25	5.00	50.00	K ₂ S ₂ O ₈	1.3	0.0003	-1.5	93.2	0.2593	0.0491
19	7	1.42	20.00	10.00	H ₂ O ₂ + K ₂ S ₂ O ₈	21.4	0.0104	45	99.9	0.765	0.1277
12	8	2.00	50.00	10.00	K ₂ S ₂ O ₈	12.2	0.0052	-13.8	97.1	0.5069	0.0288
15	9	2.00	5.00	10.00	K ₂ S ₂ O ₈	41.3	0.0173	21.5	99.6	0.9513	0.0314
5	10	2.00	5.00	50.00	H ₂ O ₂ + K ₂ S ₂ O ₈	33.2	0.0133	75.5	96.2	0.5004	0.0997
3	11	2.00	50.00	10.00	H ₂ O ₂	37.4	0.0158	18.6	99.4	0.8127	0.0598
8	12	2.00	5.00	50.00	H ₂ O ₂	31.8	0.0132	69.7	96.2	0.9447	0.0236
10	13	0.25	50.00	50.00	H ₂ O ₂	23.3	0.0093	70.5	91.7	0.35	0.059
20	14	1.42	5.00	23.33	K ₂ S ₂ O ₈	6.4	0.0022	-11.6	95.5	0.4821	0.0262
27	15	0.25	5.00	50.00	H ₂ O ₂ + K ₂ S ₂ O ₈	4.5	0.0017	65.6	90.9	0.31	0.0339
13	16	0.25	50.00	10.00	H ₂ O ₂ + K ₂ S ₂ O ₈	5.7	0.0022	48	95.9	0.3084	0.0677
26	17	0.25	5.00	50.00	K ₂ S ₂ O ₈	0.3	0.0001	-4.8	88.5	0.1723	0.0492
21	18	0.25	35.00	23.33	K ₂ S ₂ O ₈	2.9	0.0012	-14.5	95.7	0.3278	0.0587
27	19	2.00	50.00	10.00	H ₂ O ₂ + K ₂ S ₂ O ₈	19.9	0.0084	35.2	99.5	0.5439	0.0975
22	20	0.83	50.00	36.67	H ₂ O ₂ + K ₂ S ₂ O ₈	12.6	0.0053	45.8	98.6	0.4533	0.0784
17	21	0.25	5.00	50.00	H ₂ O ₂ + K ₂ S ₂ O ₈	0.3	0.0001	60.2	90.1	0.3455	0.0235
1	22	2.00	5.00	50.00	K ₂ S ₂ O ₈	4.4	0.0018	1.5	95.6	0.5067	0.0203
14	23	0.25	50.00	50.00	K ₂ S ₂ O ₈	5.4	0.0019	-2.2	95.8	0.3	0.0655
2	24	0.25	5.00	10.00	H ₂ O ₂	25.2	0.012	72.1	99.4	0.7105	0.0557
16	25	2.00	50.00	50.00	H ₂ O ₂ + K ₂ S ₂ O ₈	9.3	0.0029	67.1	98	0.4409	0.0659
6	26	0.25	5.00	50.00	H ₂ O ₂ + K ₂ S ₂ O ₈	19.1	0.0073	67.6	99.1	0.48	0.0951
25	27	2.00	50.00	10.00	H ₂ O ₂	30.9	0.0138	18.2	99.3	0.7754	0.0451

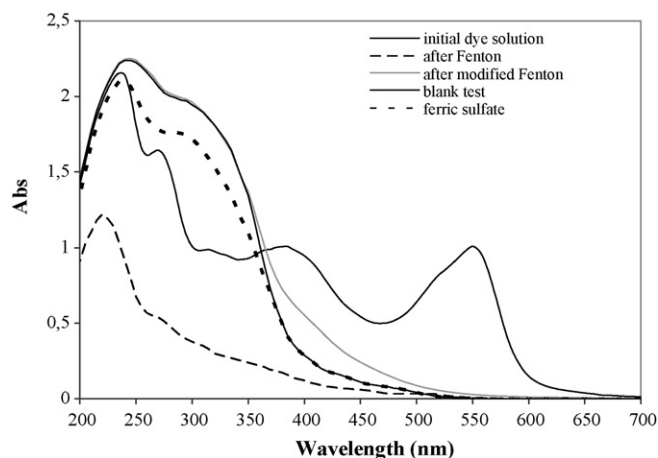


Fig. 1. UV-vis absorption spectra of initial dye solution; $\gamma_{RV2} = 50 \text{ mg L}^{-1}$, $\gamma_{RY3} = 50 \text{ mg L}^{-1}$; after 30 min of Fenton, $\text{Fe}^{2+}/\text{H}_2\text{O}_2$, and modified Fenton oxidation, $\text{Fe}^{2+}/\text{K}_2\text{S}_2\text{O}_8$, with $[\text{Fe}^{2+}] = 2.00 \text{ mmol L}^{-1}$ and oxidant/catalyst ratio of 5.00, in comparison with spectra obtained for blank test ($\text{Fe}^{2+}/\text{K}_2\text{S}_2\text{O}_8$) and ferric sulfate.

negligible absorptivity on wavelength of maximum absorbance of other dye (Table 1). Absorbance spectra of initial dye solution and changes after applied oxidation processes are presented in Fig. 1. It can be seen that after Fenton oxidation, $\text{Fe}^{2+}/\text{H}_2\text{O}_2$, absorbance through visible region of spectrum is almost zero, while in UV,

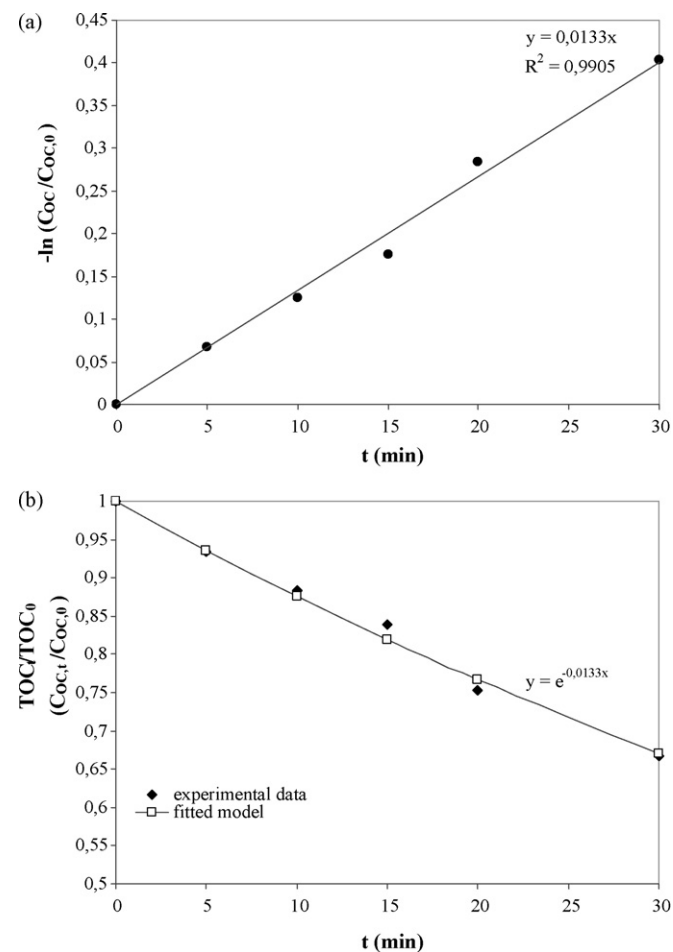


Fig. 2. (a) Pseudo-first order plot for mineralization of the initial dye solution; (b) non-linear curve fit to the TOC data obtained at oxidation times ranging from 0 to 30 min; $\gamma_{RV3} = 50 \text{ mg L}^{-1}$, $[\text{Fe}^{2+}] = 2 \text{ mmol L}^{-1}$, oxidant/catalyst ratio of 5 ($\text{H}_2\text{O}_2 + \text{K}_2\text{S}_2\text{O}_8$).

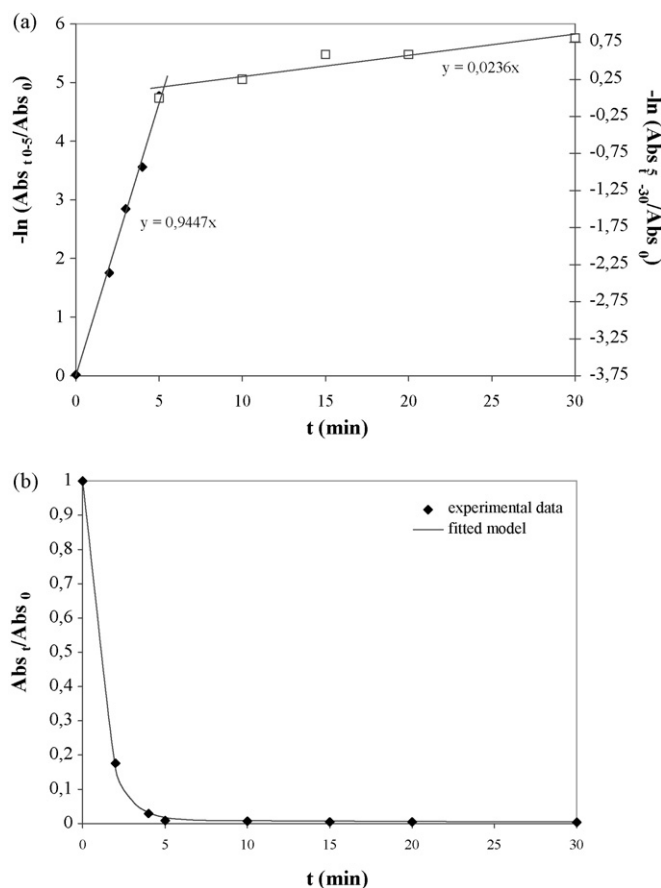


Fig. 3. (a) First-order plot for discoloration kinetics at $\lambda_{\text{maxRV2}} 550 \text{ nm}$ according to two first-order in-series reaction model; (b) non-linear curve fit to the absorbance data; $\gamma_{RV3} = 50 \text{ mg L}^{-1}$, $[\text{Fe}^{2+}] = 2.00 \text{ mmol L}^{-1}$, oxidant/catalyst ratio of 5.00 ($\text{H}_2\text{O}_2 + \text{K}_2\text{S}_2\text{O}_8$).

it was decreased significantly, implying that both dyes, RV2 and RY3 were degraded to colorless products. After applying modified Fenton oxidation, $\text{Fe}^{2+}/\text{K}_2\text{S}_2\text{O}_8$, absorbance on $\lambda_{\text{maxRV2}} 550 \text{ nm}$ is around zero, implying on an abatement of initial RV2 molecule. On other wavelength, $\lambda_{\text{maxRY3}} 385 \text{ nm}$, absorbance is relatively high, due to interference with species that appear during the process. Namely, in $\text{Fe}^{2+}/\text{K}_2\text{S}_2\text{O}_8$ system ferrous ions oxidize to ferric ions (Eq. (1)) and peroxydisulfate ions can react in different way resulting in a certain amount of sulfate ions [15]. Blank control test was performed with $\text{FeSO}_4 \cdot 7\text{H}_2\text{O}$ and $\text{K}_2\text{S}_2\text{O}_8$ in concentrations that correspond with the ones applied for the oxidation of dye solution. Spectrum obtained for $\text{Fe}^{2+}/\text{K}_2\text{S}_2\text{O}_8$ control test compared with the spectrum of solution of $\text{Fe}_2(\text{SO}_4)_3 \cdot 9\text{H}_2\text{O}$ was also shown in Fig. 1. The obvious match implied that Fe^{3+} and SO_4^{2-} have been produced during the process resulting in a significant absorption of light even at $\lambda_{\text{maxRY3}} 385 \text{ nm}$. Therefore, absorbance of RY3 was not isolated during the reaction due to strong interference. In case if only the absorbance of RY3 was relevant for assessing the water quality after the treatment, the hydroxides of iron could be precipitated and interference would be reduced [28]. In this particular case, the amount of iron in the treated system was equally relevant, so the absorbance at 385 nm was used not only as a measure of color abatement, but also as an indicator of the amount of iron ions in the system. The presence of color in wastewater is not acceptable in environmental manner and its removal at 385 nm was taken into account as controlled response as well.

Moreover, initial concentration of RY3 was one of the CFs that had to be evaluated through statistical model as a factor with potential effect on overall process efficiency, due to structural similarity

Table 4
ANOVA results—model validation.

Source	Sum of squares	Degrees of freedom	Mean square	F	p	R ²
Y₁						
Model	3892.45	10	389.25	27.27	<0.0001	0.9446
Total	4120.87	26	–	–	–	–
Residual	228.42	16	14.28	–	–	–
Lack of fit	197.08	11	17.92	2.86	0.1281	–
Pure error	31.34	5	6.27	–	–	–
Y₂						
Model	7.7 × 10 ⁻⁴	16	14.8 × 10 ⁻⁵	33.20	<0.0001	0.9815
Total	7.9 × 10 ⁻⁴	26	–	–	–	–
Residual	1.5 × 10 ⁻⁵	10	1.5 × 10 ⁻⁵	–	–	–
Lack of fit	1 × 10 ⁻⁵	5	2 × 10 ⁻⁶	1.98	0.2358	–
Pure error	5 × 10 ⁻⁶	5	1 × 10 ⁻⁶	–	–	–
Y₃						
Model	29455.64	14	2103.97	39.03	<0.0001	0.9785
Total	30102.55	26	–	–	–	–
Residual	646.91	12	53.91	–	–	–
Lack of fit	483.92	7	69.13	2.12	0.2125	–
Pure error	162.99	5	32.60	–	–	–
Y₄						
Model	238.89	9	26.54	9.47	<0.0001	0.8337
Total	286.56	26	–	–	–	–
Residual	47.67	17	2.80	–	–	–
Lack of fit	35.89	12	2.99	1.27	0.4220	–
Pure error	11.78	5	2.36	–	–	–
Y₅						
Model	1.21	10	0.12	18.60	<0.0001	0.9208
Total	1.32	26	–	–	–	–
Residual	0.10	16	7 × 10 ⁻³	–	–	–
Lack of fit	0.098	11	9 × 10 ⁻³	2.32	0.1968	–
Pure error	7 × 10 ⁻³	5	1 × 10 ⁻³	–	–	–
Y₆						
Model	0.017	14	1 × 10 ⁻³	12.13	<0.0001	0.9340
Total	0.018	26	–	–	–	–
Residual	1 × 10 ⁻³	12	1 × 10 ⁻⁴	–	–	–
Lack of fit	8 × 10 ⁻⁴	7	1 × 10 ⁻⁴	1.23	0.4248	–
Pure error	4 × 10 ⁻⁴	5	9 × 10 ⁻⁵	–	–	–

with RV2 and its contribution to TOC content of dye solution. The effect that caused presence of RY3 will be discussed in Section 3.3.

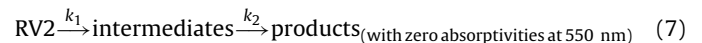
3.2. Kinetic studies

The residual TOC concentration was monitored over a 30-min period and a mineralization rate (TOC removal) was modeled using Eq. (6)

$$\frac{-dC_{OC}}{dt} = k_m C_{OC} \Rightarrow \frac{C_{OC}}{C_{OC,0}} = e^{-k_m t} \quad (6)$$

regarding the general mass balance for a well-mixed, constant volume and constant temperature batch reactor, with the following boundary conditions; $t=0$, $C_{OC}=C_{OC,0}$. In Eq. (1), k_m is the reaction rate constant, referred hereafter as apparent mineralization rate constant (min^{-1}), C_{OC} is the TOC concentration (mg L^{-1}), and $(-dC_{OC}/dt)$ is the first order mineralization (removal) rate. In order to determine the apparent mineralization rate constant, $-\ln(C_{OC}/C_{OC,0})$ was plotted against the reaction time (Fig. 2a). A non-linear curve fit to the TOC data was also performed according to Eq. (6) and the apparent mineralization rate was confirmed, $k_m = 0.0133 \text{ min}^{-1}$, respectively (Fig. 2b). Furthermore, discoloration kinetics and respective rates were investigated as well. First, it was checked if dye degradation by Fenton oxidation could be described by first-order kinetics as it was established for photocatalytic oxidation [31,32]. The semilog data plot of absorbance vs. time, as shown in Fig. 3a, did not produce a single straight line. Therefore, a simple first-order model was not suitable for describing the entire period of oxidation. However, the semilog

plot indicated two regions, suggesting a two first-order in-series reaction model, as described by Eq. (7) [33,34]



Assuming that both reactions followed a first-order kinetics, the batch model for the concentration of studied dye, C_{RV} , and of the intermediates, C_{CI} , with time could be described by Eqs. (8) and (9), with the following boundary conditions; $t=0$, $C_{RV2} = C_{RV2,0}$, $C_{CI} = 0$.

$$\frac{-dC_{RV2}}{dt} = k_1 C_{RV2} \Rightarrow \frac{C_{RV2}}{C_{RV2,0}} = e^{-k_1 t} \quad (8)$$

$$\frac{dC_{CI}}{dt} = k_1 C_{RV2} - k_2 C_{CI} \Rightarrow C_{CI} = \left[\frac{k_1 C_{RV2,0}}{k_2 - k_1} \right] (e^{-k_1 t} - e^{-k_2 t}) \quad (9)$$

Measured absorbances are the sum of contributions from the dyes and intermediates. With that in mind, Eqs. (8) and (9) could be combined with Lambert–Beer's law giving the following equation, Eq. (10):

$$\frac{\text{Abs}_t}{\text{Abs}_0} = e^{-k_1 t} + \left(\frac{\varepsilon_{CI}}{\varepsilon_{RV2}} \right) \left[\frac{k_1}{(k_2 - k_1)} \right] e^{-k_1 t} - e^{-k_2 t} \quad (10)$$

where ε_{RV2} and ε_{CI} represents molar extinction coefficients of RV2 and intermediates, respectively, and Abs_t represents the absorbance measured in time at the wavelength of interest (550 nm).

Furthermore, some simplifications of the first-order in-series reaction model were made. Regarding the knowledge of Fenton oxidation's high efficiency due to the fast and constant generation of hydroxyl radicals, it could be assumed that after 5 min,

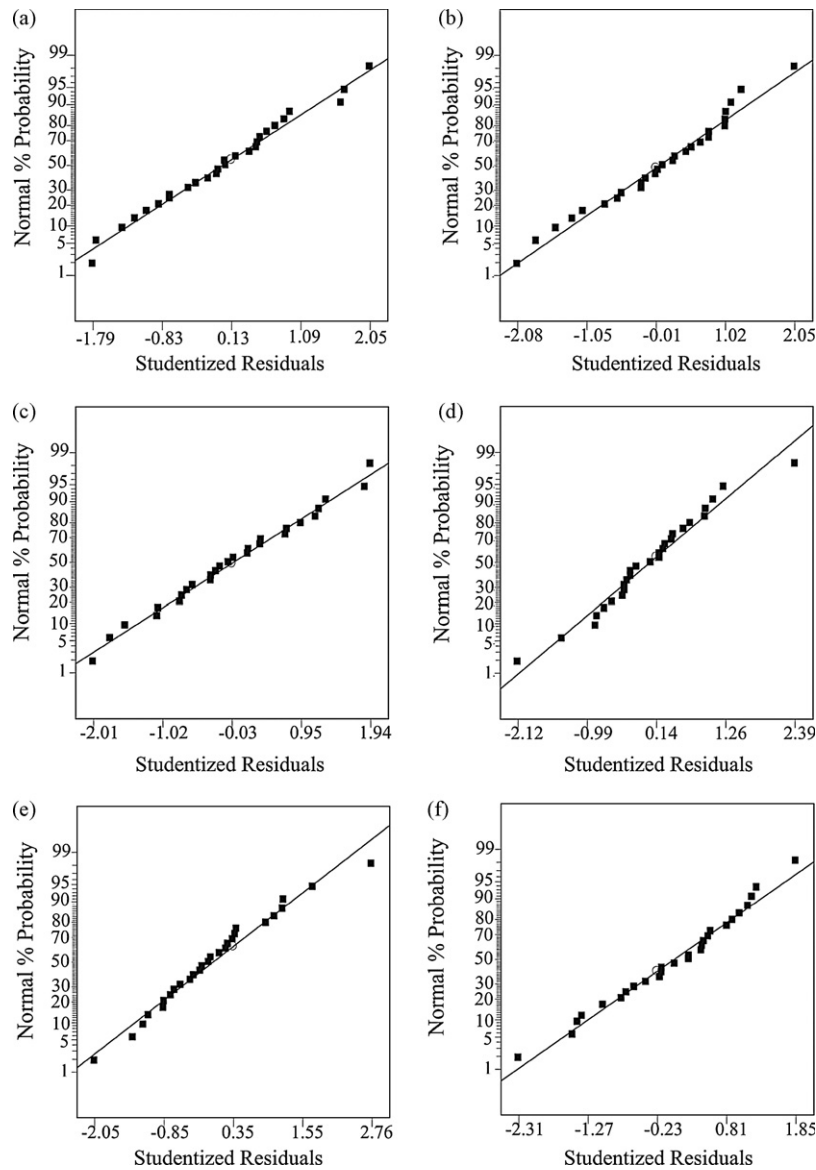


Fig. 4. Normal probability plot of residuals for each response: (a) Y_1 , percentage of total TOC removal, (b) Y_2 , apparent mineralization rate constant, k_m , min^{-1} ; percentages of total color removal (c) at λ_{maxRV3} 385 nm, Y_3 , (d) at λ_{maxRV2} 550 nm, Y_4 , and apparent discoloration rate constants; (e) k_1 , min^{-1} , Y_5 , (f) k_2 , min^{-1} , Y_6 .

concentration of studied dye, RV2, became negligible compared to intermediates concentration, leading to the fact that measured absorbance in fifth minute of the process depended only on concentration of intermediates. Moreover, oxidation occurred after fifth minute could be considered as stand-alone process of intermediates degradation. In first 5 min, concentration of RV2 is eligible and due to the high molar extinction coefficient of RV2 at 550 nm, it could be stated that absorbance is contributed solely by RV2. These statements were described as follows, Eqs. (11) and (12):

$$\frac{\text{Abs}_{t \rightarrow 5}}{\text{Abs}_0} = e^{-k_1 t} \quad (11)$$

$$\text{Abs}_{5 \text{ min}} \equiv \text{Abs}'_0 \Rightarrow \frac{\text{Abs}_{t \rightarrow 30}}{\text{Abs}'_0} = e^{-k_2 t} \quad (12)$$

Finally, $-\ln(\text{Abs}_t/\text{Abs}'_0)$ were plotted against the reaction time to determine the apparent discoloration rate constants (Fig. 3b).

It was also performed a non-linear curve fit to the absorbance data according to Eq. (10) (Fig. 3c), and kinetic parameters, k_1 and k_2 , as well as the ratio $\varepsilon_{\text{Cl}}/\varepsilon_{\text{RV2}}$, were estimated. Values obtained by previously described simplified model were used as starting

points. It was assumed that the ratio $\varepsilon_{\text{Cl}}/\varepsilon_{\text{RV2}}$ could be identified with the ratio of absorbance in the fifth minute and initial one, $\text{Abs}_5/\text{Abs}_0$, according to Lambert–Beer's law. Namely, in the fifth minute TOC value was not decreased significantly so it could be approximated that the concentration of intermediates in the fifth minute of the reaction was equal to the initial concentration of RV2. These statements are expressed by the following equation, Eq. (13):

$$C_{\text{RV2},0} \approx C_{\text{Cl},5} \Rightarrow \frac{\varepsilon_{\text{Cl}}}{\varepsilon_{\text{RV2}}} \approx \frac{\text{Abs}_5}{\text{Abs}_0} \quad (13)$$

The value for the ratio $\varepsilon_{\text{Cl}}/\varepsilon_{\text{RV2}}$ that fitted in a full first-order in-series reaction model was around 0.01. Apparent discoloration rate constants, k_1 and k_2 , 0.9447 min^{-1} and 0.0236 min^{-1} , respectively, obtained by using the simplified model, showed no bias when used in non-linear curve fit according to the full first-order in-series model (Fig. 3c).

3.3. Statistical analyses and interpretation

The statistical study of the process was performed using response surface methodology (RSM), particularly by a D-optimal

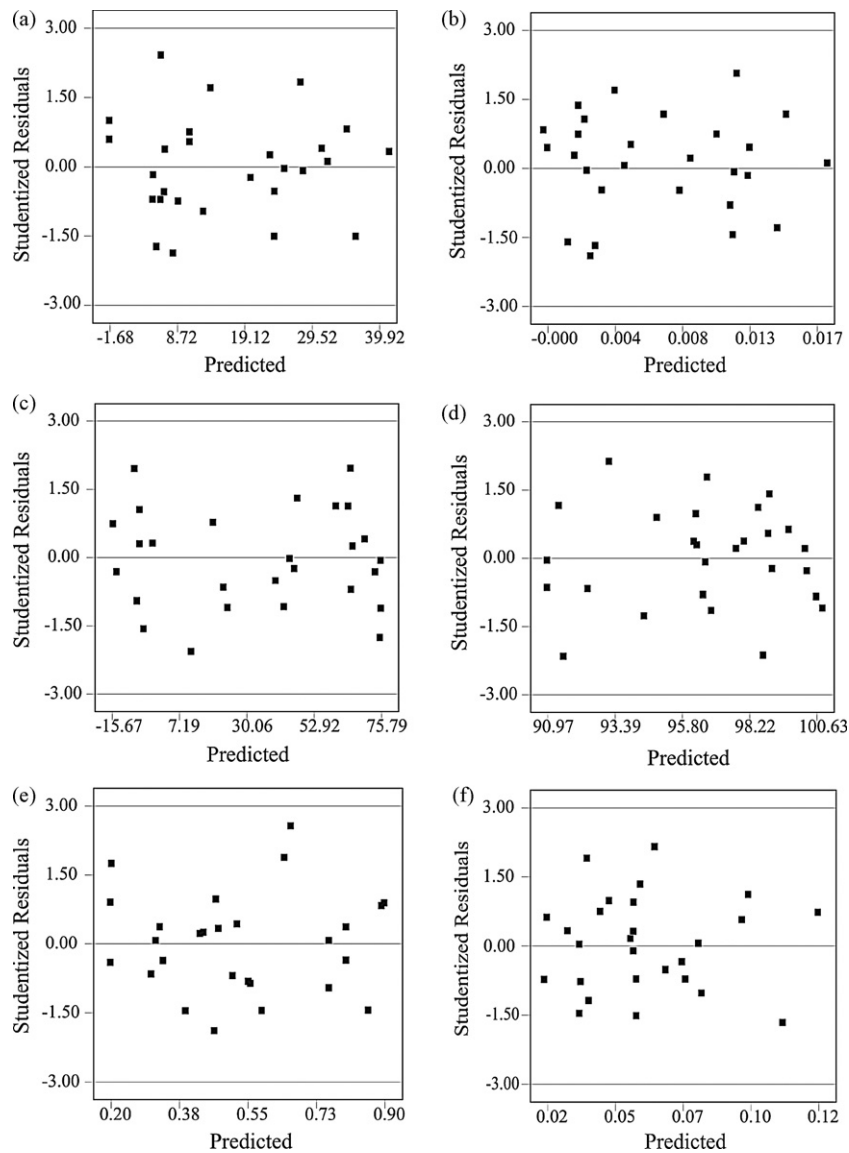


Fig. 5. Residuals vs. predicted plot for each response: (a) Y_1 , percentage of total TOC removal, (b) Y_2 , apparent mineralization rate constant, k_m , min^{-1} ; percentages of total color removal (c) at λ_{maxRY3} 385 nm, Y_3 , (d) at λ_{maxRV2} 550 nm, Y_4 , and apparent discoloration rate constants: (e) k_1 , min^{-1} , Y_5 , (f) k_2 , min^{-1} , Y_6 .

design since this design could deal with categorical factors easily. Individual parameters and their interaction effects on TOC and color removal, the apparent mineralization and discoloration rate constants were determined and statistical models of process were developed.

Multiple regression analysis of experimental data, performed using Design-Expert software, resulted with model equations describing dependency of responses (Y_1 , Y_2 , Y_3 , Y_4 , Y_5 , Y_6) to four process parameters and some of their interactions. Some of the responses did not fit well in a proposed reduced cubic model and, therefore, further modifications were made: (i) some terms were deleted transforming the reduced cubic model to modified two-factor interaction (2FI) model and/or (ii) adequate quadratic terms were added, X_1^2 , $X_1^2X_2$. Full modified predictive model is described in Eq. (14):

$$\begin{aligned}
 Y = & b_0 + b_1X_1 + b_2X_2 + b_3X_3 + \beta_1X_4 + \beta_2X_4 + b_{11}X_1^2 + b_{12}X_1X_2 \\
 & + b_{13}X_1X_3 + \beta_{11}X_1X_4 + \beta_{12}X_1X_4 + b_{23}X_2X_3 + \beta_{21}X_2X_4 \\
 & + \beta_{22}X_2X_4 + \beta_{31}X_3X_4 + \beta_{31}X_3X_4 + \beta_{32}X_3X_4 + b_{112}X_1^2X_2 \quad (14)
 \end{aligned}$$

where β_{ij} represents coefficients for categorical factor or their interactions with numerical factors.

For current study each response surface model were evaluated using ANOVA (Table 4). For each model equation F -values in range from 12.13 to 49.40 imply that the models are significant. Obtained R^2 values are close to one suggesting the fit is good and a variation in the observed values can be explained by the chosen model. The examination of residuals was used to investigate the model adequacy. Fig. 4a–f present a normal probability plot of residuals for each response, Y_1 , Y_2 , Y_3 , Y_4 , Y_5 , Y_6 . In each case there is no severe indication of non-normality and neither any evidence pointing to possible outliers. Normal plots presented in Fig. 4a–f are normally distributed and resemble a straight line. Also, residuals are structureless and contain no obvious patterns, so it can be concluded that the models are adequate. Furthermore, residuals vs. predicted plots are normally distributed and the equality of variance does not seem to be violated, as presented in Fig. 5a–f.

Effects of factors and their interactions on responses Y_1 , Y_2 , Y_3 , Y_4 , Y_5 and Y_6 are presented in Table 5 according to predictive model in coded terms obtained by modifying Eq. (5), as presented in Eq.

Table 5
RSM regression coefficients for each response.

Term	p						Coefficient	Regression coefficient					
	Y ₁	Y ₂	Y ₃	Y ₄	Y ₅	Y ₆		Y ₁	Y ₂ (10 ⁻³)	Y ₃	Y ₄	Y ₅	Y ₆
Constant							<i>b</i> ₀	17.19	8.2	36.79	98.30	0.65	0.066
X ₁	<0.0001	<0.0001	0.0032	0.0021	<0.0001	0.5534	<i>b</i> ₁	5.01	2.4	-4.65	1.36	0.098	1 × 10 ⁻³
X ₂	0.1598	0.0137	0.2476	0.0322	0.0471	0.0916	<i>b</i> ₂	-1.66	2.7	-1.19	0.88	-0.036	0.024
X ₃	0.0003	<0.0001	0.0006	0.0001	0.0060	<0.0001	<i>b</i> ₃	-4.17	-2.1	10.34	-1.63	-0.055	-0.013
X ₄	<0.0001	<0.0001	<0.0001	0.0663	<0.0001	<0.0001	<i>β</i> ₁ , <i>β</i> ₂	11.45; -1.47	5.2; -1.0	23.41; 17.55	0.71; 0.13	0.21; -0.078	-0.011; 0.022
X ₁ ²	-	0.4181	-	0.0445	0.0196	0.1856	<i>b</i> ₁₁	-	-1.2	-	-2.22	-0.13	-0.010
X ₁ X ₂	0.0070	0.0080	0.1897	-	-	0.2563	<i>b</i> ₁₂	-2.70	-0.96	2.75	-	-	-3 × 10 ⁻³
X ₁ X ₃	-	0.2582	0.0020	0.0087	0.1595	-	<i>b</i> ₁₃	-	-0.1	8.15	1.14	0.029	-
X ₁ X ₄	0.0058	0.0019	0.0009	-	-	<0.0001	<i>β</i> ₁₁ , <i>β</i> ₁₂	-0.42; 4.19	-0.5; 2.1	-12.02; 4.91	-	-	-0.012; 0.026
X ₂ X ₃	-	0.5254	0.2879	-	0.2934	-	<i>b</i> ₂₃	-	0.04	-2.16	-	-0.023	-
X ₂ X ₄	0.0066	0.0030	0.0195	-	0.0822	0.0015	<i>β</i> ₂₁ , <i>β</i> ₂₂	1.85; -4.29	1.1; -2.2	-1.97; -5.82	-	-0.039; -0.021	0.01; -0.016
X ₃ X ₄	-	0.5374	0.1855	0.0539	-	0.0038	<i>β</i> ₃₁ , <i>β</i> ₃₂	-	0.2; -0.6	4.53; -3.73	-1.11; -0.22	-	4 × 10 ⁻³ ; -0.014
X ₁ ² X ₂	-	0.0058	-	-	-	0.0356	<i>b</i> ₁₁₂	-	-4.0	-	-	-	-0.023

Table 6
Model equations for each observed response.

Response	Equation
<i>H</i> ₂ O ₂ used as an oxidant	
<i>k</i> _m , min ⁻¹	0.014 - 0.007 [Fe ²⁺] - 8 × 10 ⁻⁵ (ox/Fe) - 9 × 10 ⁻⁵ γ _{RY3} + 0.005[Fe ²⁺] ² + 5 × 10 ⁻⁴ [Fe] (ox/Fe) - 7 × 10 ⁻⁶ [Fe] γ _{RY3} + 1 × 10 ⁻⁷ (ox/Fe) γ _{RY3} - 2 × 10 ⁻⁴ [Fe ²⁺] ² (ox/Fe)
<i>k</i> ₁ , min ⁻¹	0.702 + 0.456 [Fe ²⁺] - 0.002 (ox/Fe) - 0.003γ _{RY3} - 0.175 [Fe ²⁺] ² + 0.002 [Fe] γ _{RY3} - 5 × 10 ⁻⁵ (ox/Fe) γ _{RY3}
<i>k</i> ₂ , min ⁻¹	0.067 - 0.061 [Fe ²⁺] - 2 × 10 ⁻⁵ (ox/Fe) - 5 × 10 ⁻⁴ γ _{RY3} + 0.024 [Fe ²⁺] ² + 3 × 10 ⁻³ [Fe] (ox/Fe) - 1 × 10 ⁻³ [Fe ²⁺] ² (ox/Fe)
Equimolar mixture of H ₂ O ₂ + K ₂ S ₂ O ₈ used	
<i>k</i> _m , min ⁻¹	0.009 - 0.004 [Fe ²⁺] - 2 × 10 ⁻⁴ (ox/Fe) - 1 × 10 ⁻⁴ γ _{RY3} + 0.005 [Fe ²⁺] ² + 5 × 10 ⁻⁴ [Fe] (ox/Fe) - 7 × 10 ⁻⁶ [Fe] γ _{RY3} + 5 × 10 ⁻⁷ (ox/Fe) γ _{RY3} - 2 × 10 ⁻⁴ [Fe ²⁺] ² (ox/Fe)
<i>k</i> ₁ , min ⁻¹	0.391 + 0.456 [Fe ²⁺] - 0.001 (ox/Fe) - 0.003γ _{RY3} - 0.175 [Fe ²⁺] ² + 0.002 [Fe] γ _{RY3} - 5 × 10 ⁻⁵ (ox/Fe) γ _{RY3}
<i>k</i> ₂ , min ⁻¹	0.109 - 0.017 [Fe ²⁺] - 1 × 10 ⁻³ (ox/Fe) - 1 × 10 ⁻³ γ _{RY3} + 0.024 [Fe ²⁺] ² + 3 × 10 ⁻³ [Fe] (ox/Fe) - 1 × 10 ⁻³ [Fe ²⁺] ² (ox/Fe)
K ₂ S ₂ O ₈ used as an oxidant	
<i>k</i> _m , min ⁻¹	0.005 - 0.009 [Fe ²⁺] - 7 × 10 ⁻⁵ (ox/Fe) - 8 × 10 ⁻⁵ γ _{RY3} + 0.005 [Fe ²⁺] ² + 5 × 10 ⁻⁴ [Fe] (ox/Fe) - 7 × 10 ⁻⁶ [Fe] γ _{RY3} + 1 × 10 ⁻⁷ (ox/Fe) γ _{RY3} - 2 × 10 ⁻⁴ [Fe ²⁺] ² (ox/Fe)
<i>k</i> ₁ , min ⁻¹	0.238 + 0.456 [Fe ²⁺] - 0.003 (ox/Fe) - 0.003γ _{RY3} - 0.175 [Fe ²⁺] ² + 0.002 [Fe] γ _{RY3} - 5 × 10 ⁻⁵ (ox/Fe) γ _{RY3}
<i>k</i> ₂ , min ⁻¹	0.065 - 0.064 [Fe ²⁺] - 2 × 10 ⁻⁴ (ox/Fe) - 1 × 10 ⁻⁴ γ _{RY3} + 0.024 [Fe ²⁺] ² + 3 × 10 ⁻³ [Fe] (ox/Fe) - 1 × 10 ⁻³ [Fe ²⁺] ² (ox/Fe)

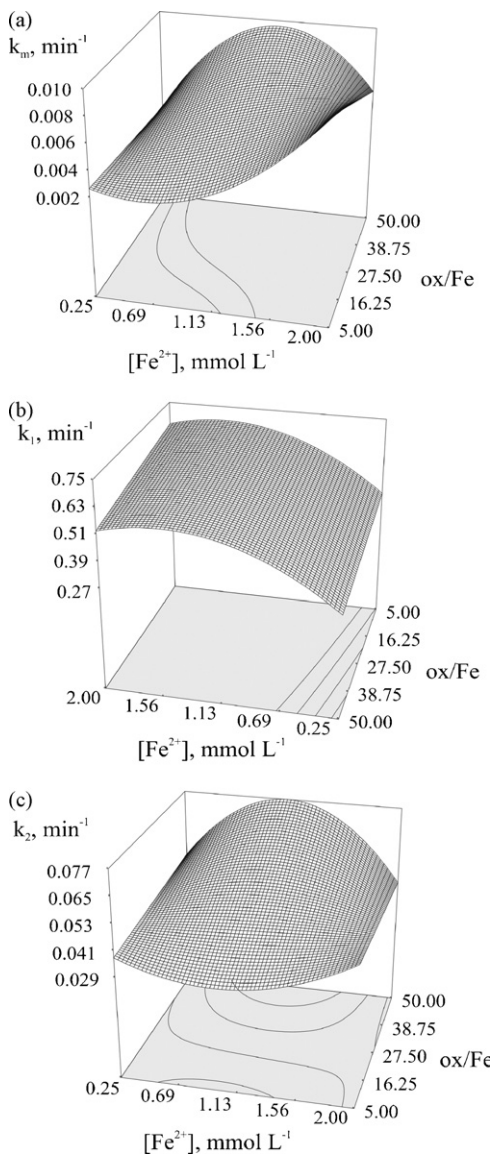


Fig. 6. Graphical interpretations of the models obtained for the (a) apparent mineralization rate constant, (b) and (c) apparent discoloration rate constants with average responses regarding type of oxidant presented; $\gamma_{RY3} = 50 \text{ mg L}^{-1}$, $[\text{Fe}^{2+}] = 2 \text{ mmol L}^{-1}$.

(14). For a significant term in each predictive model, p -value is less than 0.1000 (Table 5). Coded equation is useful for identifying the relative significance of the factors by comparing the factor coefficients, because comparison cannot be made with the actual equation due to the scaling of coefficients to accommodate the units of each factor. On the other hand, coefficients for multi-level categorical factor (X_4) or their interactions with numerical factors (e.g. X_1X_4), β_{ij} , are not as simple to interpret, since they do not have a physical, but only a mathematical meaning. Namely, β_1 is the difference of the second level (in this particular case, when as oxidant mixture $\text{H}_2\text{O}_2 + \text{K}_2\text{S}_2\text{O}_8$ is used) from the overall average; β_2 is the difference of a third level (oxidant is $\text{K}_2\text{S}_2\text{O}_8$) from the overall average, and the negative sum of the coefficients will be the difference of the first level from the overall average. Therefore, these coefficients could not be used for interpretation of the models, yet real impression about process performance could be achieved from graphical interpretation of the models.

In this work, a special emphasis was put on kinetics, so a final response surface predictive models given in actual terms regard-

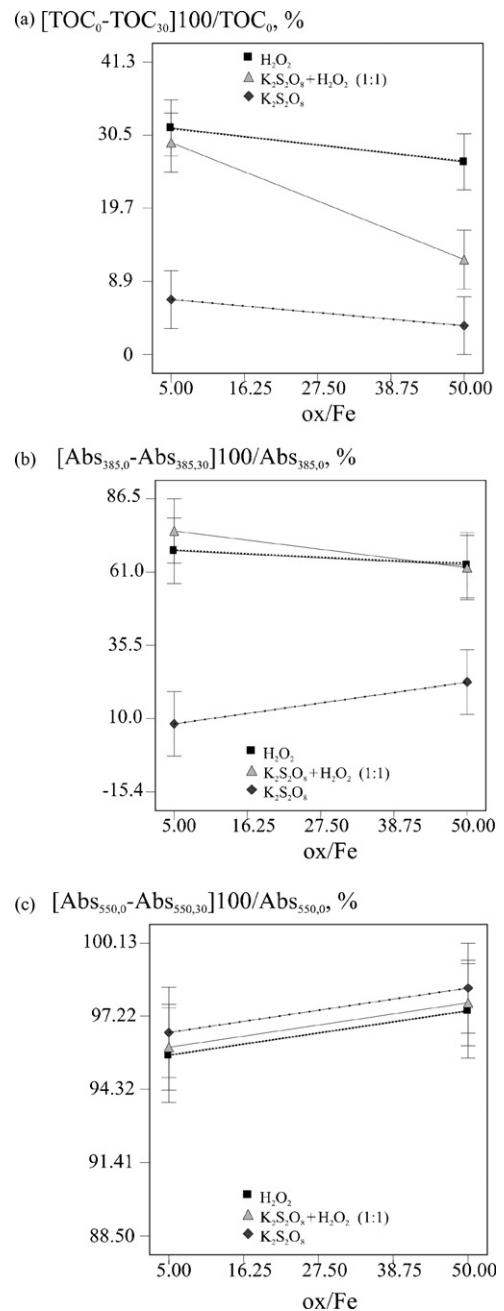


Fig. 7. Performance of applied processes in terms of (a) TOC, (b) and (c) color removal; $\gamma_{RY3} = 50 \text{ mg L}^{-1}$, $[\text{Fe}^{2+}] = 2 \text{ mmol L}^{-1}$; a two-factor interaction plot.

ing responses Y_2 (actual; $k_m, \text{ min}^{-1}$), Y_5 (actual $k_1, \text{ min}^{-1}$) and Y_6 (actual $k_2, \text{ min}^{-1}$) are stated in Table 6. Since each combination of categorical levels has an equation that predicts the response, three equations are presented for each apparent rate constant. Graphical interpretations of these models are presented in Fig. 6a–c, taking into consideration average responses regarding type of oxidant used.

In terms of TOC and color removal, insight to process performance could be gained from graphical interpretation of models (Fig. 7a–c), where each response is presented as a function of oxidant/catalyst molar ratio (ox/Fe). Furthermore, presented responses assume initial concentration of ferrous ions, $[\text{Fe}^{2+}]$, of 1.13 mmol L^{-1} , i.e. in the middle of the investigated concentration range, and maximal initial RY3 concentration, γ_{RY3} , i.e. 50 mg L^{-1} ,

in order to obtain the highest organic load. It can be seen that the highest mineralization and discoloration rates were achieved when H_2O_2 is used as an oxidant. Performance of classic Fenton process is very good even when ratio catalyst/oxidant is rather low. When modified Fenton reagent is applied ($\text{Fe}/\text{H}_2\text{O}_2 + \text{K}_2\text{S}_2\text{O}_8$ or $\text{K}_2\text{S}_2\text{O}_8$) higher ratio catalyst/oxidant is needed. Furthermore, the presence of RY3 effected the discoloration at 550 nm in great extent as it can be also seen from Table 5. A significant effect of initial RY3 concentration on discoloration at 550 nm confirmed a fact that a presence of similar pollutant in the system would significantly slower down degradation of RV2 and its intermediates due to competitiveness towards oxidizing radicals, $\bullet\text{OH}$, $\text{S}_2\text{O}_8^{\bullet-}$ and $\text{SO}_4^{\bullet-}$.

4. Conclusion

The mineralization and discoloration of dye solution containing RV2 and RY3 by Fenton, $\text{Fe}^{2+}/\text{H}_2\text{O}_2$, and modified Fenton oxidation, $\text{Fe}^{2+}/\text{H}_2\text{O}_2 + \text{K}_2\text{S}_2\text{O}_8$, $\text{Fe}^{2+}/\text{K}_2\text{S}_2\text{O}_8$, were studied. RSM D-optimal design was applied. Four factors have been examined, including (X_1) initial Fe^{2+} concentration, (X_2), initial oxidant/catalyst ratio, i.e. ox/Fe , (X_3), initial RY3 concentration, γ_{RY3} , and finally, categorical factor, (X_4), type of used oxidant, H_2O_2 , $\text{H}_2\text{O}_2 + \text{K}_2\text{S}_2\text{O}_8$ (1:1) or $\text{K}_2\text{S}_2\text{O}_8$.

Using kinetic and statistical analysis of the applied processes, where appeared almost 100% of color removal, as monitored at λ_{maxRV2} 550 nm, and up to approximately 40% of initial TOC were removed after 30 min, the following was noticed: (i) initial RY3 concentration is the significant factor with a great influence on RV2 and its intermediates degradation resulting in more faint removal of color (550 nm) and TOC, (ii) among applied oxidants, H_2O_2 was found to be most appropriate, (iii) the optimal reagents doses for reducing the pollutant content, in terms of TOC and color removal were assessed for each applied process, pointing to the initial concentration of ferrous ions in the middle of the investigated range; $[\text{Fe}^{2+}] = 1.13 \text{ mmol L}^{-1}$, and oxidant/catalyst molar ratio at higher levels, starting from 27.5, (iv) RV2 kinetic behavior in applied systems was described and (v) the apparent rate constants were determined. Considering assessed optimal operating conditions and the highest initial organic load, i.e. concentrations of both dyes of 50 mg L^{-1} , mineralization was described by pseudo-first-order kinetics with observed rate constant $k_m = 0.0133 \text{ min}^{-1}$. A kinetic model describing discoloration was composed of two first-order in-series reactions with discoloration rates; $k_1 = 0.9447 \text{ min}^{-1}$ and $k_2 = 0.0236 \text{ min}^{-1}$. As a result of performed statistical analysis, apparent rate constants were presented as a function of three factors, X_1 , X_2 , X_3 and their relevant interactions at each level of fourth, categorical factor, X_4 , i.e. depending which oxidant was used.

From the results obtained in this study, it can be concluded that the given predictive models described the studied systems very well and satisfactory throughout the investigated range, evaluated by the analysis of variance analysis, ANOVA. Although this study implied the simplified description of the treated system on macro level, and also assessing the processes' efficiency regarding to the corresponding reaction rate constants, obtained results are eligible and the used statistical method is recommendable.

Acknowledgement

This work was supported by the Croatian Ministry of Science, Education and Sport, Project #125-1253092-1981.

References

- [1] M. Muruganandham, M. Swaminathan, Advanced oxidative decolourisation of Reactive Yellow 14 azo dye by UV/TiO₂, UV/H₂O₂, UV/H₂O₂/Fe²⁺ processes—a comparative study, *Sep. Purif. Technol.* 48 (2005) 297–303.
- [2] J.H. Ramirez, C.A. Costa, L.M. Madeira, Experimental design to optimize the degradation of the synthetic dye Orange II using Fenton's reagent, *Catal. Today* 107–108 (2005) 68–76.
- [3] J.M. Chacón, M.T. Leal, M. Sánchez, E.R. Bandala, Solar photocatalytic degradation of azo-dyes by photo-Fenton process, *Dyes Pigm.* 69 (2006) 144–150.
- [4] R. Nilsson, R. Nordlinder, U. Wass, B. Meding, L. Belin, Asthma, rhinitis, and dermatitis in workers exposed to reactive dyes, *Brit. J. Ind. Med.* 50 (1993) 65–70.
- [5] C. Hessel, C. Allegre, M. Maisseu, F. Charbit, P. Moulin, Guidelines and legislation for dye house effluents, *J. Environ. Manag.* 83 (2007) 171–180.
- [6] T. Robinson, G. McMullan, R. Marchant, P. Niagam, Remediation of dyes in textile effluent: a critical review on current treatment technologies with a proposed alternative, *Bioresour. Technol.* 77 (2001) 247–255.
- [7] E. Forgas, T. Cserháti, G. Oros, Removal of synthetic dyes from wastewaters: a review, *Environ. Int.* 30 (2004) 953–971.
- [8] R.S. Gupta, Environmental Engineering and Science, An Introduction, Government Institutes, Rockville, 1997.
- [9] P.K. Malik, S.K. Sanyal, Kinetics of decolourisation of azo dyes in wastewater by UV/H₂O₂ process, *Sep. Purif. Technol.* 36 (2004) 167–175.
- [10] V.K. Gupta, Suhas, Application of low-cost adsorbents for dye removal—a review, *J. Environ. Manag.* 90 (2009) 2313–2342.
- [11] S. Papić, N. Koprivanac, A. Lončarić Božić, A. Meteš, Removal of some reactive dyes from synthetic wastewater by combined Al(III) coagulation/carbon adsorption process, *Dyes Pigm.* 62 (2004) 291–298.
- [12] H. Jirankova, J. Cakl, O. Markvartova, P. Dolecek, Combined membrane process at wastewater treatment, *Sep. Purif. Technol.* 58 (2007) 299–303.
- [13] S. Karcher, A. Kornmüller, M. Jekel, Anion exchange resins for removal of reactive dyes from textile wastewaters, *Water Res.* (2002) 4717–4724.
- [14] H.Y. Shu, M.C. Chang, H.J. Fan, Decolorization of azo dye acid black 1 by the UV/H₂O₂ process and optimization of operating parameters, *J. Hazard. Mater.* 113 (2004) 201–208.
- [15] J. Levec, Wet oxidation processes for treating industrial wastewaters, *Chem. Biochem. Eng. Q* 11 (1997) 47–58.
- [16] M. Muruganandham, M. Swaminathan, Decolourisation of reactive orange 4 by Fenton and photo-Fenton oxidation technology, *Dyes Pigm.* 63 (2004) 315–321.
- [17] S.G. Huling, B.E. Pivetz, In situ chemical oxidation. U.S. Environmental Protection Agency, Office of Research and Development, National Risk Management Research Laboratory, 2006, EPA/600/R-06/072.
- [18] C. Liang, C.J. Bruell, M.C. Marley, K.L. Sperry, Persulfate oxidation for in situ remediation of TCE-1. Activated by ferrous ion with and without a persulfate-thiosulfate redox couple, *Chemosphere* 55 (2004) 1213–1223.
- [19] E. Ferrarese, G. Andreottola, I.A. Oprea, Remediation of PAH-contaminated sediments by chemical oxidation, *J. Hazard. Mater.* 152 (2008) 128–139.
- [20] T.K. Lau, W. Chu, N.J.D. Graham, The aqueous degradation of butylated hydroxyanisole by UV/S₂O₈²⁻: study of reaction mechanisms via dimerization and mineralization, *Environ. Sci. Technol.* 41 (2007) 613–619.
- [21] K. Clarke, R. Edge, E.J. Land, S. Navaratnam, T.G. Truscott, The sulphate radical is not involved in aqueous radiation oxidation processes, *Rad. Phys. Chem.* 77 (2008) 49–52.
- [22] R.H. Myers, D.C. Montgomery, Response Surface Methodology. Process and Products Optimization Using Designed Experiments, John Wiley & Sons Inc., New York, 2002.
- [23] F.N.A. López, M.C.D. Quintana, A.G. Fernández, The use of a D-optimal design to model the effects of temperature, NaCl, type and acid concentration on *Lactobacillus pentosus* IGLAC01, *J. Appl. Microbiol.* 101 (2006) 913–926.
- [24] K. Bernaerts, K.P.M. Gysemans, T. Nhan Minh, J.F. Van Impe, Optimal experimental design for cardinal values estimation: guidelines for data collection, *Int. J. Food Microbiol.* 100 (2005) 153–165.
- [25] W.L. Poston, E.J. Wegman, J.L. Solka, D-optimal design methods for robust estimation of multivariate location and scatter, *J. Stat. Plan. Infer.* 73 (1998) 205–213.
- [26] N. Koprivanac, D. Vujević, Degradation of an azo dye by Fenton type processes assisted with UV irradiation, *Int. J. Chem. Reactor Eng.* 5 (2007) A56.
- [27] I. Grčić, M. Mužić, D. Vujević, N. Koprivanac, Evaluation of atrazine in UV/FeZSM-5/H₂O₂ system using factorial experimental design, *Chem. Eng. J.* 150 (2009) 476–484.
- [28] I. Grčić, D. Vujević, N. Koprivanac, Modeling the mineralization and discoloration in colored systems by (US)Fe²⁺/H₂O₂/S₂O₈²⁻ processes: a proposed degradation pathway, *Chem. Eng. J.* (2009), doi:10.1016/j.cej.2009.10.042.
- [29] B. Muthukumari, K. Selvam, I. Muthuvel, M. Swaminathan, Photoassisted hetero-Fenton mineralisation of azo dyes by Fe(II)-Al₂O₃ catalyst, *Chem. Eng. J.* 153 (2009) 9–15.
- [30] S. Ray, J.A. Lalman, N. Biswas, Using the Box–Benken technique to statistically model phenol photocatalytic degradation by titanium dioxide nanoparticles, *Chem. Eng. J.* 150 (2009) 15–24.

- [31] K. Tanaka, K. Padermpole, T. Hisanaga, Photocatalytic degradation of commercial azo dyes, *Water Res.* 34 (2000) 327–333.
- [32] V.V. Tarasov, G.S. Barancova, N.K. Zaitsev, Z. Dongxiang, Photochemical kinetics of organic dye oxidation in water, *Process Saf. Environ. Prot.* 81 (2003) 243–249.
- [33] R.B.M. Bergamini, E.B. Azevedo, L.R. Raddi de Araújo, Heterogeneous photocatalytic degradation of reactive dyes in aqueous TiO₂ suspensions: decolorization kinetics, *Chem. Eng. J.* 149 (2009) 215–220.
- [34] A.J. Julson, D.F. Ollis, Kinetics of dye decolorization in an air–solid system, *Appl. Catal. B: Environ.* 65 (2006) 315–325.